Radboud University Nijmegen

Faculty of Science

Department of High Energy Physics

Simulating Random Triangulations

Finding a Planck scale in 2d Quantum Gravity Simulations

Thesis BSc Physics and Astronomy

Author:
Anna van Asselt

Supervisor:
dr. Timothy Budd

Second reader:
dr. Frank Filthaut

July 2022

Abstract

This thesis discusses the asymptotic safety theory in Quantum Gravity and its implication that the geometry of spacetime should become fractal and scaling invariant at high energies and thus at small distance scales, in particular at distances smaller than the Planck scale. It does so by looking at a 2d toy model to describe the transition in geometry that is analogous to the transition that happens at the Planck scale. In this model, a flat triangulation will be evolved by a Markov chain Monte Carlo simulation which creates a uniformly distributed triangulation by performing flips on a grid of triangles. This transition gives a timescale in the simulation. Using finite size scaling it was determined what the critical exponent of the time in this simulation was. The result is within previously known boundaries and gives visually the expected results.

Contents

1 Introduction

In 1915 Einstein published his work on General Relativity. It states that massive bodies curve spacetime, which results in the pull of gravity as we know it. This theory has passed many experimental tests over time, but one of the main problems is that we currently cannot properly describe what happens if we combine it with quantum mechanics. This is one of the main open problems in physics.

One of the proposed solutions is to look at the geometry of spacetime, at scales where quantum effects are significantly strong enough, as a fractal and scale-invariant geometry. This thesis will take a look at a model for this geometry in 2 dimensions using triangulations, specifically at the moment of transition to a fractal geometry, this is characterised by the critical exponent. This is a property of the model that has not been studied in detail before. It has been studied mathematically, but this has only resulted in lower and upper bounds that leave quite a bit of room. This thesis will use a Monte Carlo simulation to numerically compute the critical exponent. The result can help us learn more about the model.

This thesis will describe how the problem arises in quantum field theory and one of the possible solutions to this in section 2. The research discussed in this thesis made use of 2d toy model describing this solution, which will be discussed in detail in section 2 and 4. The results of the research on the toy model will be shown and discussed in section 5.

2 Background Theory

General relativity

General relativity (GR) dictates that the effects of gravity that we detect in physics come from the fact that masses and other forms of energy curve spacetime. This can be visualised by a picturing a table cloth flatly suspended in air, with a bowling ball placed on it, making a dent. Gravity then exhibits itself in the way a small marble would now roll towards the bowling ball along the table cloth. In this famous metaphor, spacetime is the table cloth. When Einstein was researching his theory, one of the biggest obstacles to overcome was how to translate the visual image of the table cloth to mathematics. The solution turned out to be a mathematical notation: tensors.
This thesis will not dive too deep into the mathematical background of tensors, but it is important to discuss one specific kind of tensor: the metric $g_{\mu\nu}$. This is the specific kind of tensor used to describe spacetime geometry. The metric can be applied to two vectors to give the inner product between the two. It can be used to describe the distance travelled in spacetime

$$ds^2 = g_{\mu\nu} dx^\mu dx^\nu. \tag{1}$$

Where the indices μ and ν run over the three spatial coordinates and the time coordinate. In the metric, these axes differ in sign. The distances that follow from this equation describe the proper time of a worldline through spacetime. In flat Minkowski spacetime the metric $g^{\mu\nu}$ would not have any effect in this equation. In a curved spacetime, however, it can cause the total distance travelled to be different from what it would be in flat spacetime. This affects the shortest paths through a spacetime. The paths of free falling objects (also called geodesics) are therefore effected as well. This causes the gravitational effects in a spacetime. In a flat spacetime, the geodesics would be straight lines, meaning there are no gravitational effects in such a spacetime. Besides geodesics, another important equation to mathematically describe gravity are the Einstein equations

$$R_{\mu\nu} - \frac{1}{2} R g_{\mu\nu} = 8\pi G T_{\mu\nu}. \tag{2}$$

The left side of this equation describes the curvature of the metric, the right side uses the stress-energy tensor $T_{\mu\nu}$ to describe energy in the universe. This equation thus describes how energy influences curvature.[1]

2.1 From classical to quantum mechanical

To see how gravity could be united with quantum mechanics, let's first take a look at how a classical theory can be written as a quantum mechanical theory in general. This is done by computing the action S, which is an integral over the (classical) Lagrangian of the particle.

$$S = \int \mathrm{d}^4x \, \mathcal{L} \tag{3}$$

Classically, one has to find stationary points to find solutions. In quantum mechanics, however, the solutions are found by taking $e^{iS/\hbar}$ and then taking the path integral over every possible path[2, 3]. This is in the general case of quantum mechanics in Minkowski space. Through a a formal analytic continuation of the time coordinate t to imaginary time $\tau = it$, called Wick rotation, the Minkowski metric turns into a (4d) Euclidean metric while at the same time the term $e^{iS/\hbar}$ turns into $e^{-S/\hbar}$. As will be explained in section 3, we consider Euclidean metrics, so in this specific case the term $e^{-S/\hbar}$ would actually be used.

$$Z = \int \mathcal{D}x \, e^{-S[x(t)]/\hbar}. \tag{4}$$

The term $e^{-S/\hbar}$ then gives a real weight to every path, which allows us to interpret Z as a statistical sum over all paths with $e^{-S/\hbar}$ as unnormalised probabilities.
This can also be done for a field, instead of a single particle, in which case the path can be described as a configuration in spacetime. One property of $e^{iS/\hbar}$ is that $|e^{iS/\hbar}| = 1$ for all S, however, non-stationary points will destructively interfere with each other. Consequently, only the weights corresponding to the stationary points will be non-zero. This makes the theory in the classical limit consistent with the classical theory.

Quantizing gravity

We can now take a look at what will happen if we try to quantize general relativity. The paths where the integral runs over will again be a configuration of dynamical spacetime. In the context of GR these paths are all possible metrics, modulo diffeomorphisms. These are all possible metrics that cannot be written as each other using a coordinate transformation.

$$\int \mathcal{D}g_{\mu\nu} e^{iS[g_{\mu\nu}]/\hbar} \tag{5}$$

The natural choice of action which can be derived from the Einstein equations is the Einstein-Hilbert action.

$$S_{EH} = \int \mathrm{d}^d x \sqrt{|g|} R \tag{6}$$

The fact that we work modulo diffeomorphisms causes the integration to get very complicated. The solution to work around this complicated integration is to find a way to write the configurations of spacetime independent of coordinates. This can be done by using simplices [1] as building blocks for spacetime. Geometries built like this are called triangulations, which will be explained more in section 3. These triangulations will replace the integral over all possible configurations with a summation over all possible triangulations[4, 5]. To do this, the action S should also be adapted to these discredited triangulations, so we retrieve the path integrals with the Einstein-Hilbert action if we take the size of the triangles to 0 and the number of triangles to infinity. While modelling triangulations, it is therefore important to remember that if we take the number of triangles N to infinity, the model corresponds to real configurations of spacetime.

There are different ways to sum over all triangulations. This depends on the weights that we associate with each triangulation. In the context of this research, we take the statistical sum over all triangulations uniformly. This means that every triangulation has the same chance to form as any other. The reason we use uniformly distributed triangulations comes from the Gauss–Bonnet theorem in 2d[6]. This states that the action in the path integral will only depend on the topology

$$S[g_{\mu\nu}(x)] = 4\pi - 4\pi g. \tag{7}$$

With g the genus[2]. This means that all triangulations will have the same weight in the integral. Therefore all triangulations should have the same chance of being formed.

2.2 Renormalisation

If we only take the path integral over metrics that are close to flat Euclidean space, and then apply perturbation theory on the result, we will retrieve a summation of Feynman diagrams. This would allow us to compute observables with arbitrary precision, if were it not for the existence of loop Feynman diagrams. In the summation of the Feynman

[1] In 2d, these are triangles.
[2] As will be discussed later, we will use a torus, so $g = 1$

diagrams, higher order Feynman diagrams will have loops in them. There is an infinite integral over the loop momenta in a Feynman diagram, which will lead to infinities in the summation. This will result in theoretical infinities in measurable quantities, where experiments clearly measure finite numbers.
To illustrate the solution to this discrepancy, let's first introduce some terminology. There are masses and coupling constants in the Lagrangian, we'll call these *bare* couplings. We can experimentally measure these quantities, we'll call those *physical* couplings. The result obtained above includes infinities because it is naively assumed that the bare quantities are equal to physical quantities. However, if we let that restriction loose, we can use renormalisation to choose the bare quantities such that the physical outcomes will agree with experiments.[7]

Running of Couplings

The result of this renormalisation, so the values of the bare couplings, depends on the energy scale, this is called running of couplings. Concretely this means, for example, that the coupling strength of an electron will depend on the energy scale at which you measure it. Running of couplings can be seen as a flow[3], following a path as a function of the energy scale. For the other three fundamental forces besides gravity, this path can be seen in figure 1. The energy scale runs on the x-axis, the inverse of the strength of the couplings on the y-axis. Once the flow for a force is known, the renormalisation only has to be executed at one point in the theory space of energy to know the rest of the results, since the rest can be deduced from the flow. There is one important property of this flow for it to become physical, which is that the quantities of dimensionless couplings cannot go to infinity as the energy scales become large. This means that only points in theory space of bare quantities corresponding to a flow that will converge to a fixed point can be physical.
There are two possibilities for this fixed point, it can be zero or finite. If it is zero, the theory is called asymptotically free. This is what happens for the couplings of QCD, the strong force, as can be seen in figure 1 (note the inverse of the y-axis). In that case, all coupling constants will become zero in high energies, so there can be no interactions.

We know however, from the fact that gravity is not perturbatively renormalisable[8] that fixed points equal to zero are not allowed for gravity. The other option for this fixed point is for it to be equal to a finite number unequal to zero. In this case, the theory is called asymptotically safe.[9]

2.3 The asymptotic safety scenario

The physical idea behind such a fixed point is that at high energies, it does not matter what your energy is exactly, all physics can be described by the same effective action. This also means that for small distance scales (high energy) the exact distance should not matter as well. The consequence of this is that the effect of gravity, which is represented by the spacetime, will have to be scale invariant at small distance scales.
The first solution to this is that spacetime will be flat at small distance scales. This would be a very easy and nice solution. However, on flat spacetime, no gravitational effects can take place. This practically means that the couplings will have to go to zero, so this spacetime belongs to the asymptotic free theory. We therefore need to find a spacetime that is scaling invariant and not flat, to research asymptotic safe theory. Such a spacetime is found in the other option for a scaling invariant spacetime: a fractal spacetime. Fractal spacetimes have no well-defined notion of curvature, are not flat

[3]This is called functional renormalisation group flow

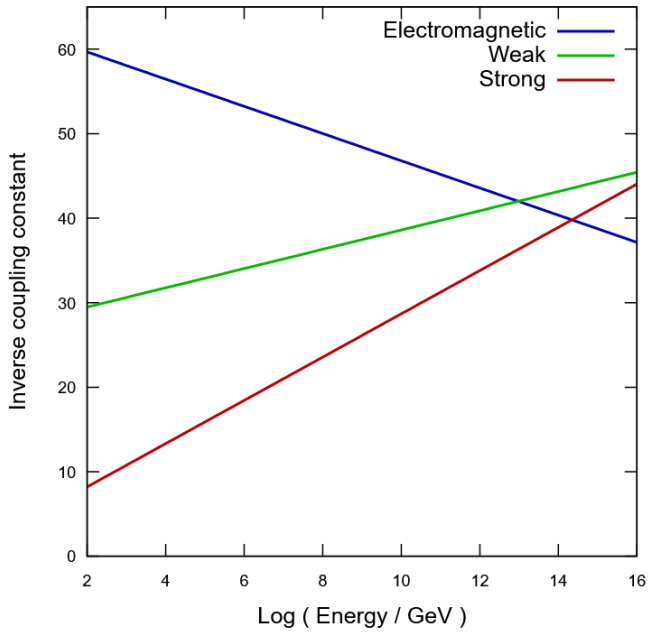

Figure 1: The running of couplings for the three fundamental forces besides gravity[10].

and can be scaling invariant. We can therefore make the following statement: in the asymptotically safe scenario, spacetime is such that at large distance scales it will be flat or locally flat, to remain a solution to GR, at small distance scales it will be fractal and scaling invariant. The scale at which the transition takes place is called the Planck scale[7]

$$\ell_{\mathrm{P}} = \sqrt{\frac{\hbar G}{c^2}} \approx 1.6 \cdot 10^{-35}\,\mathrm{m}. \tag{8}$$

This is equal to the scale at which quantum effects become visible for the gravitational force. The scaling invariance of this new spacetime is what sets it apart from the spacetime on larger scales, as we expect these to change at scales comparable to the Planck scale.

3 Geometry beyond the Planck scale

The asymptotic safety theory described in section 2.3 results in new behaviour of the geometry beyond the Planck scale. The path integral quantization from section 2.1 allows us to approximate the geometry of these spacetimes as triangulations. In the following section, let's take a look at these triangulations describing fractal geometries in more detail.

3.1 2d Toy model

Triangulations model the geometry using triangles as building blocks. These geometries can describe metrics with both spatial dimensions as time dimensions. For example, to describe a 2+1 dimensional geometry, one can make use of causal dynamical triangulations. These triangulations achieve 3 dimensions, using 3d building blocks and then implementing a time axis through the one of the spatial axes[5].
This thesis however, will focus on a toy model of 2d quantum gravity (so only spatial dimensions), to specifically look for the analogy of the Planck scale in this model. The model actually has two Planck scales, just like how the real Planck scale can be expressed in different units than distances. One is the distance scale, wherein zooming in enough should give a random, fractal and scale invariant triangulation back. The other Planck scale can be found in the time[4] it takes to create these triangulations that can model the geometry found beyond the Planck scale.

Time scales in the triangulations

The triangulations are updated using a Monte Carlo simulation. In figure 2 this process is illustrated. The simulation starts from a grid of N equilateral[5] triangles, with N a finite number, as can be seen in figure 2a. We give the grid periodic boundary conditions so that it forms a torus. The periodic boundary conditions mimic a grid with an infinite number of triangles. This is necessary since the model is based on triangulations with an infinite amount of triangles.
The simulation then performs flips on the triangles in the grid. During flips, two adjacent triangles are taken randomly. The edge that they both share is then flipped to the two corners that they did not share yet, like in figure 2b. Doing this many times on random edges will alter the grid such that the successive triangulations are drawn from the uniform distribution, as can be seen in figure 2c. This allows us to get truly random triangulations. One can then define the time the simulations runs, as the amount of flips that have been done at the time of measurement.
In this thesis, the terminology of sweeps, t, will be used, wherein one sweep will be equal to N flips. This terminology is chosen because then after taking one sweep, every triangle will have been flipped once flipped once on average. This allows us to compare the times of different sized triangulation more properly. Finding the Planck scale in the time scale of the simulations thus requires us to know how many sweeps are necessary to create a uniform triangulation. This amount of sweeps will be referred to as the mixing time τ. To properly define τ, we first need to introduce the critical exponent.

This is done as follows: we start with an infinite regular triangulation at $t_i = 0$. This triangulation can then become a random triangulation by performing $t = t_f$ sweeps of triangle flips. We then hypothesise that there exists an exponent $\alpha > 0$ such that the

[4] More precisely: the number of Monte Carlo steps, but we will call this time in the thesis. Do not confuse this with the time in spacetime! In our model, we only have spatial dimensions.

[5] In this thesis, the edges are not plotted as having the same length. This is because the plots are embedded in the 2d flat space.

geometry of the triangulation has a well-defined limit when t_f goes to infinity if we take the side lengths of the triangles to be $t_f^{-\frac{1}{4\alpha}}$. This limit should then describe a random continuous metric on the 2-dimensional plane. Upon zooming in, it should approach the (scale-invariant) random metric of pure 2d quantum gravity. Upon zooming out it should approach the metric of the flat Euclidean plane.

Now we can define a hypothesis from the general theory of Markov Chain Mixing time.

$$\lim_{N\to\infty} \frac{\log(\tau)}{\log(N)} = \alpha. \tag{9}$$

From mathematical background [11, 12, 13], we know that the critical exponent α is bounded like

$$\frac{1}{4} \leq \alpha \leq \frac{9}{2}. \tag{10}$$

Combining these two equations allows us to make the following hypothesis.

$$\tau \approx N^{\alpha} \tag{11}$$

With $N \gg 1$ and with α the critical exponent.

If N would go to infinity, the correct measurement of τ could be found. Using this simulation, however, N will have to be a finite number. To still make an educated estimate of τ, the finite size scaling technique will be applied, which will be discussed in the next section.

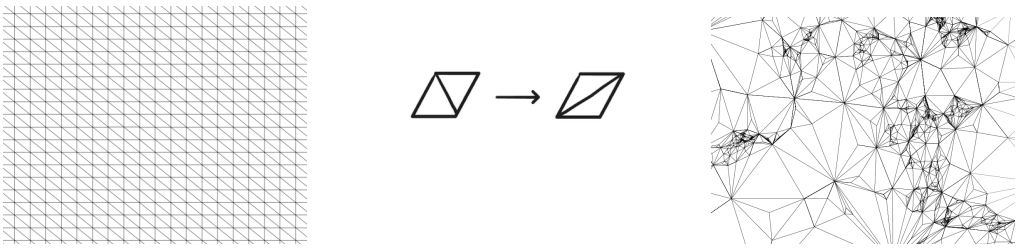

(a) A regular grid of N triangles.

(b) A "flip" performed on two triangles.

(c) A randomised uniform distribution.

Figure 2: The simulations runs flips over the grid of triangles.

3.2 Approximating α

To find the mixing time, one must therefore find the critical exponent α. It can be found by using finite size scaling, which uses the fact that N cannot be infinite. To perform finite size scaling, one first needs to find a relation between α and other measurable quantities. This research made use of distances to achieve this.

Distances in the triangulation

Distances between vertexes in the triangulations are measured using the fact that the edges are defined as having a unit length. Therefore we can use the least amount of edges between two vertices as a length measurement. The reason distances can be used

to find α is because uniform triangulations have a very distinct mathematical property.

In 2d Euclidean geometry the area of the set of all points within distance r (a disk) is given by $A \sim r^2$. However, in fractals the area scales as

$$A \sim r^{d_{\text{Hausdorff}}}. \tag{12}$$

The Hausdorff dimension is a attribute of a fractal. For a uniformly drawn triangulation it is generally equal to 4[14], giving

$$A \sim r^4. \tag{13}$$

If we use the amount of vertices as a measurement of the area, we can therefore check using distances when the triangulations are drawn from a uniform distribution.

When measuring distances, we measure the shortest distance to all vertices starting from a random point. This is explained in more detail in section 4.1. Effectually this means that we can measure how many vertices lie on the circumference of a circle with the radius equal to the measured distance. In flat geometry, this number would increase as $\sim r$. This is different in the geometry of uniform triangulations, where the number typically grows as $\sim r^3$.

Using this definition of distances, we can now take a look at the triangulation after a time $t \leq \tau$ sweeps. At this point in the simulation, the triangulation will resemble that of 2d quantum gravity at small distance scales, but it will still be evenly distributed at large distance scales. This leads to the hypothesis that the geometry within the geodesic distance ξ is approximately uniform, but at large distances it is still regular. Starting from a vertex, all other vertices on geodesic distance ξ will form a circle. This can be visualised by assuming that the triangulation is made up of evenly distributed circles, in which the triangles are randomly distributed, as can be seen in figure 3. These circles will all have the same radius ξ. We now suppose that ξ will grow as t. Within these circles we can use equation (13) to give a relation for the number of triangles inside the circle

$$n \approx c\,\xi^4. \tag{14}$$

With c a constant. If we now look at the case of $t = \tau$, the entire triangulation needs to be approximately uniform. Therefore $N = n$. Using equation (11) this gives: $\xi(\tau) \approx \tau^{\frac{1}{4\alpha}}$. We can now take the general case and retrieve

$$\xi(t) \approx t^{\frac{1}{4\alpha}}. \tag{15}$$

Now if one takes a histogram of the distances in the triangulation between two vertices, we would expect this histogram to reflect this behaviour as well. Since taking this histogram is effectively the same as measuring the amount of triangles at distance r away from a vertex, one would expect the histogram to grow as $\sim r^3$ at small r, and as $\sim r$ at large r, as can be seen in figure 4. The transition point would then be at $r = \xi$. The behaviour of the histogram can then be described by the following relation

$$\rho(r) = C\xi^2 \frac{r^3}{\xi^2 + r^2}. \tag{16}$$

wherein $\rho(r)$ corresponds to the value of the histogram at r and C a constant.
The function is constructed such that

$$\rho(r) = \begin{cases} Cr^3 & \text{if } r \ll \xi \\ C\xi^2 r & \text{if } r \gg \xi \end{cases}. \tag{17}$$

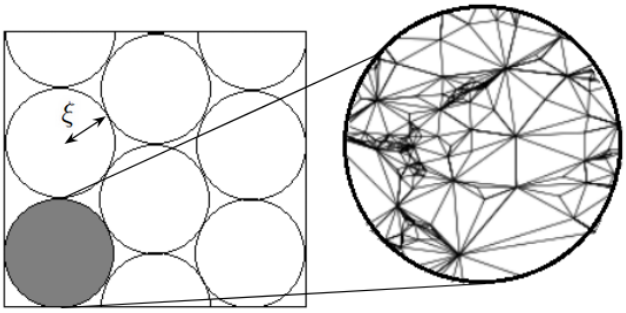

Figure 3: An approximation of the triangulation after t sweeps.

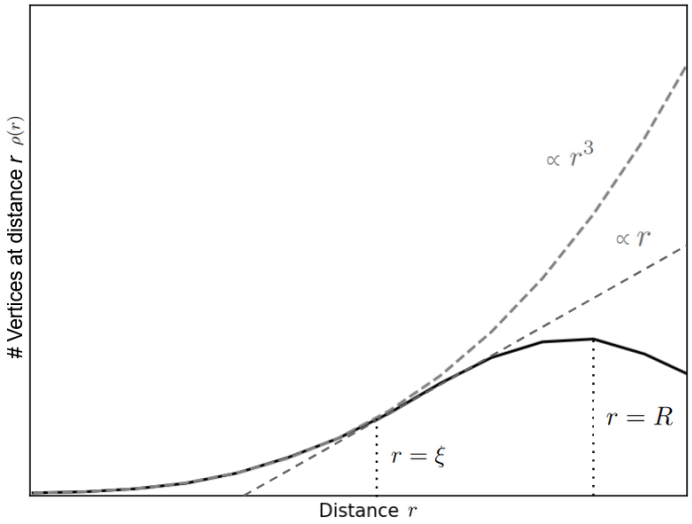

Figure 4: Example graph showing the amount of vertices at distance r from one random vertex in the triangulation, with fits showing the behaviour of the curve as r increases.

This is where the advantage of only being able to have finite N comes in to play. If N were infinite, the curve would increase linearly as r increases forever. However, because N is finite, this linearity cannot go on forever. We therefore can expect to see the curve drop off after a certain distance $r = R$, making R essentially the diameter of the system, as can also be seen in figure 4. This value can now be used by integrating ρ over r from 0 to R. This should then be roughly equal to N. This gives us:

$$N \approx \begin{cases} \displaystyle\int_0^R Cr^3 \, \mathrm{d}r = \frac{C}{4}R^4 & \text{if } R \ll \xi \\ \displaystyle\int_0^R C\xi^2 r \, \mathrm{d}r = \frac{C\xi^2}{2}R^2 & \text{if } R \gg \xi \end{cases} \tag{18}$$

Which together with equation (15) then leads to:

$$R \approx \begin{cases} (\frac{4N}{C})^{\frac{1}{4}} & \text{if } R \ll \xi \\ (\frac{2N}{C\xi^2})^{\frac{1}{2}} = \sqrt{\frac{2N}{C}} t^{-\frac{1}{4\alpha}} & \text{if } R \gg \xi \end{cases} \tag{19}$$

This can be summarised as:

$$R \sim N^{\frac{1}{4}} f(tN^{-\alpha}) \tag{20}$$

Where f is an unknown function with known limits

$$\lim_{t \to 0} f(t) = \frac{2}{C}^{1/2} t^{-\frac{1}{4\alpha}} \tag{21}$$

$$\lim_{t \to \infty} f(t) = \frac{4}{C}^{1/2}. \tag{22}$$

3.3 Collapse

Equation (20) can be used to compute the critical exponent α if one can obtain a graph containing all three other variables in it. This can be achieved by creating a plot like figure 4 for different amount of sweeps. By then taking the value of r that is measured most often, meaning the maximum of the graph, one can create a graph of R against t, the amount of sweeps. This can then be done for multiple N, to create more graphs that can be compared to each other. An example of such a graph can be seen in figure 5. All these graphs then follow the relation from equation (20), the only thing that keeps them from perfectly aligning is the fact that N appears in this relation. Therefore, if we would divide the terms with N out of the equation, effectively rescaling the axes, the graphs should perfectly align. After rescaling, plotting $RN^{-\frac{1}{4}}$ on the y-axis against $tN^{-\alpha}$ should result in all curves collapsing onto the unknown function f in the limit $N \to \infty$. This is called finite size scaling, and it is what allows us to find α by finding the best collapse. Only when the correct α is found, the graphs will collapse perfectly on top of each other.

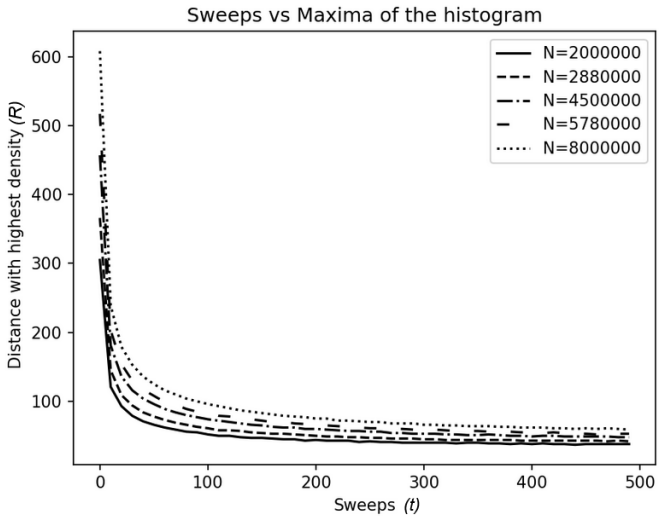

Figure 5: Graph of the most probable distance between two random vertices for triangulation with N triangles after preforming t sweeps.

4 Implementation

4.1 Simulation

The simulation that was used to create the triangulations was written in C++[6]. As described in section 3, the simulation starts with a grid of triangles with periodic boundary conditions. This grid is made by defining all edges in relation to each other. The code uses half-edges, meaning two half-edges adjacent to each other make one whole edge. This way, all triangles can be defined in half-edges separate from each other, which makes it possible to perform flips on the triangles. The flips are made in the same way, first by selecting a random edge to flip. Then the relations to the other edges are redefined to result in a triangulation with an extra flip.

The starting point of the triangulation could be checked with three properties. The first one being that the triangulation needs to be connected, that is to say, starting from one edge and only travelling along edges, an observer on the map needed to be able to reach all other edges. Secondly, to check if the triangulation itself was correct, it was checked whether the observer would always end up on any edge it started on if it would walk to the next edge three times. The last check was to calculate the genus g of the triangulation was equal to 1, as it should for any torus. This was checked using the Euler characteristic. This gave the verifiable equality

$$2 - 2 \cdot g = \#\text{Vertices} - \#\text{Edges} + \#\text{Faces} \tag{23}$$

After having checked all three for the setup of the simulation, the rest could be executed.

The simulation then uses a Markov chain Monte Carlo process to choose a random edge to flip, which is then repeated to gain the desired number of sweeps. The program can then measure distances in the triangulation and save this data in a histogram. To do so, we first need to have a uniform random vertex as a starting point to measure

[6]The codes of the simulation and the code for plotting can be found at:`https://gitlab.science.ru.nl/avasselt/code-simulating-random-triangulations`.

from[7][8]. It then performs breath-first search to assign distances to all other vertices in the triangulation. It repeats this process a chosen number of times for new random triangulations and then adds the histograms together, to reduce the statistical errors as much as possible.

4.2 Analysing the results

The simulation was carried out 9 times for five different N: $2 \cdot 10^6$, $2.88 \cdot 10^6$, $4.5 \cdot 10^6$, $5.78 \cdot 10^6$ and $8 \cdot 10^6$. Preliminary research resulted in the conclusion that values of N in this order gave smooth histograms with no visible statistical outliers. This is needed to reduce statistical errors. The specific amounts were chosen somewhat arbitrarily, with an upper limit with regards to time limitations. Each time the simulation ran, it did so for 20 times to add all that data together. In total it made 400 sweeps every time, taking snapshots for the histograms at increments of 10 sweeps. The results were then read into Python. To reduce statistical errors, the data needed to be averaged. To do this, the jackknife method was used[15]. This method takes 8 of the 9 datasets for each N and averages over these. The set left out can be changed 9 times, to create 9 sets of averaged data.

The results (still in the form of a histogram), could now be used to create a plot like figure 5, by taking the maximum of the histograms. Now to assess the quality of the collapse, we need a method to quantize the amount of overlap, as this was not possible to see by eye in much detail. This was done by interpolation of the data so that mathematical actions could be performed on it. This interpolation used the python algorithm `scipy.interpolate.interp1d`.
To compare the curves with each other, the curve with the highest N was compared with all the other curves one by one. This made it possible to compare only two curves at the same time, instead of all five at once. It was chosen to compare to the curve belonging to the highest value of N, as it is expected to satisfy equation (20) most accurately, as the equation corresponds to an infinite N.
While comparing the overlap after rescaling the axis using a certain α, the two curves were subtracted of each other, this was then squared. This was then integrated over from the minimal $tN^{-\alpha}$ that both curves share to the maximal $tN^{-\alpha}$ that both curves share. To obtain the integrated square deviation x

$$x_i = \int (R_{max}(t') - R_i(t'))^2 \, \mathrm{d}t' \,, \tag{24}$$

with $t' = tN^{-\alpha}$ and i running over the curves to compare with the curve corresponding to maximum N. This was then divided over the $tN^{-\alpha}$ that was integrated over. This is essentially taking the average over the squared difference. The integrated square deviation x could then be minimised with respect to different α, to find the α corresponding to the most overlap. This was done using the golden section search[16]. This optimisation method is based on the idea that the minimum of the curve is positioned between the two points on both sides of the point with the lowest value detected at that time in

[7]The way the simulation is structured only allows us to take a random edge and then choosing its starting vertex. We want this to be a uniformly chosen vertex, to avoid having bias to vertices connected to many edges, which would decrease the measured distances. Randomly picking any edge would result in choosing vertices with probability $\frac{d_V}{2\#e}$ with d_V the vertex degree, the amount of edges connected to the vertex, and $\#e$ the amount of edges in the triangulation. To make this probability independent of the vertex, we only accept a random vertex with a probability of $\frac{1}{d_V}$.

[8]Edges are defined using directions, to define the relations to other vertices. This way, an edge can be connected to a *next* edge and a *previous* edge. The starting vertex is then defined as the vertex that connects to the *previous* edge.

the algorithm. It uses the golden ratio to determine the distances between these points.

There is, however, still a problem when performing this minimisation. This has to do with the shape of the curve. As can be seen in figure 5, the two curves are much further apart from each other at low $tN^{-\alpha}$. This means that this part of the graph has a much higher contribution to x. This is a problem because at low t, there haven't been many sweeps performed on the triangulation. This means that the data is much more sensitive to statistical errors than it would be at larger t. There are two ways to account for this bias, both through rescaling the axes again.
The first one involves taking the logarithm of both axes. From equation (21) we can conclude that the function $f(tN^{-\alpha})$ in equation (20) will include a power law for small values of $tN^{-\alpha}$. This allows us to take the logarithm of both axes to retrieve a linear function. As can be seen in figure 6, this way, all parts of the graph will contribute equally to x.

The other solution is to take the inverse of the y-axis, to change the bias to the right part of the graph, where $f(tN^{-\alpha})$ is large, as can be seen in figure 7. To minimise the susceptibility to statistical errors, this solution would be the preferred option, this will be discussed further in section 5.2.

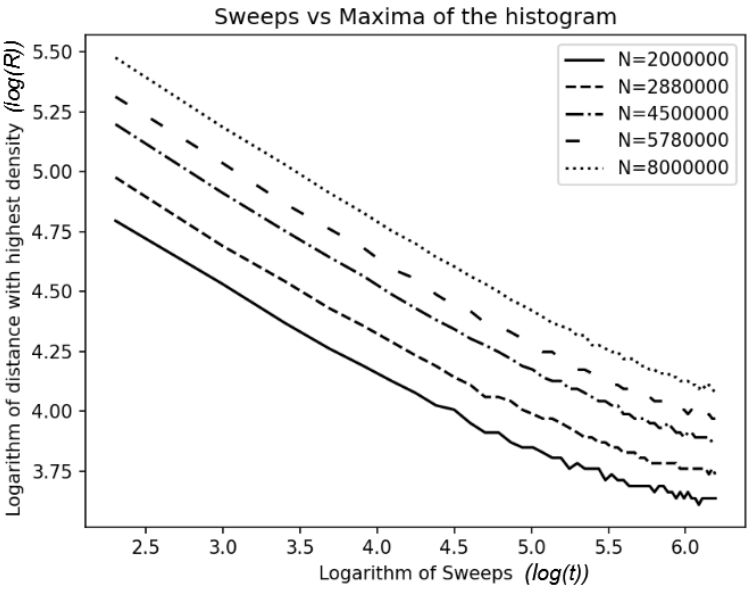

Figure 6: Graph of the maximum of the distance histogram versus the number of sweeps t, both rescaled with a logarithm.

Using one of these methods, we can obtain the critical exponent α for the four values of N compared to the highest value of N. As we expect to find the true value of α as N goes to infinity, we can expect to see the curve of α versus N converge to a constant value of α. At this point, for every N there was still 9 sets of data that resulted from the jackknife technique. The α for all these were averaged and the statistical errors were calculated using the standard deviation on these multiple data sets. This was done

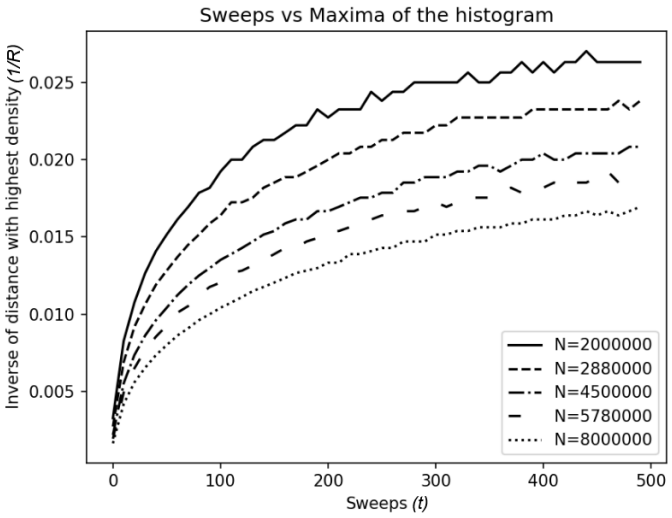

Figure 7: Graph of the maximum of the distance histogram versus the number of sweeps t, with the y-axis rescaled with an inverse.

using the jackknife standard error[17]

$$S_x = \sqrt{\frac{\sum_m (x_m - \langle x \rangle)^2}{(M-1)M}}. \tag{25}$$

These graphs can then be used to compute α with both a statistical error and a systematic error.

5 Results

5.1 Histograms

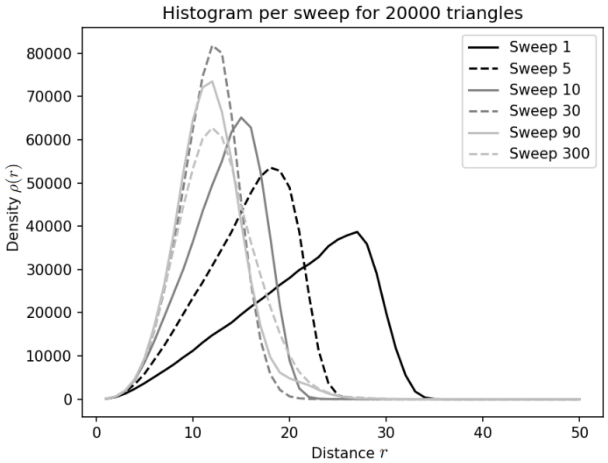

Figure 8: Histogram of the distances to other vertices, measured in units of edges, starting from a random vertex in the triangulation.

As described in section 4.1, the simulation produces histograms. It does this after a certain amount of sweeps, so it effectively produces a snapshot of the distances in the triangulations at that moment. One of the first results in this project was the creation of these histograms. They were useful to determine if the data exhibits the expected behaviour. As an example, figure 8 shows such a histogram for a relatively low amount of triangles, while still exhibiting the expected behaviour.

The histogram in figure 8 has a few notable properties. First to note is that this histogram was made of a triangulation with relatively low amount of triangles. This however does not matter, since all triangulations exhibit the same behaviour and for the purpose of this figure it was not necessary to minimise the errors be increasing N.
This universality of behaviour can also be seen in the histogram itself, as all the curves seem to follow the same pattern, even though they are not the same shape or size. This pattern is the one described in equation (16), though not as distinctive as it would be with N approaching infinity. The change of the curves as the amount of sweeps increased gave a good check if the triangulation behaved in a logical way, so by extension, a final check for the correctness of the code.

As can be seen in figure 8, the distances in the triangulation become shorter as the simulation runs. This is expected because performing the flips cause the triangulation to "crumple up", so to speak. This is because the amount of edges connected to a vertex can change during the simulation, making it possible to find shorter paths to other vertices during the simulation. After the distances become shorter, the curves start to flatten out again. This is because after a while, the triangulation can start to form "spikes", long pieces of triangulation that start to branch out from the rest.
These spikes can increase the distances in the triangulation greatly. Since the results of the simulation behave the way we expect them to, and since the triangulation satisfies the properties explained in section 4.1, this is a strong indication that the simulation works as intended.

Note on the use of R

During this thesis, the fact that all histograms have a maximum at $r = R$, was greatly used. It should however be noted that we also could have chosen to use the position of the average of the histogram, so the distance that was measured on average. Preliminary results, not shown in this thesis, showed that figure 5 qualitatively stayed the same, so with view on time constraint, the decision was made to only focus on measuring α using R. This could however be interesting to take another look at in further research, especially if this would affect the final number of α significantly.

5.2 Finding the critical exponent α

The critical exponent α was found using the graphs in figures 5, 6 and 7 as intermittent results. Using the method described in section 4.2, the results in figure 9 were obtained. Their corresponding weighted average over all N can be seen in table 1.

Table 1: Results of α for the different measuring methods.

Measuring method	No rescaling	Log-Log scaling	Inverse scaling
α	0.4800 ± 0.0008	0.5579 ± 0.0015	0.5307 ± 0.0018

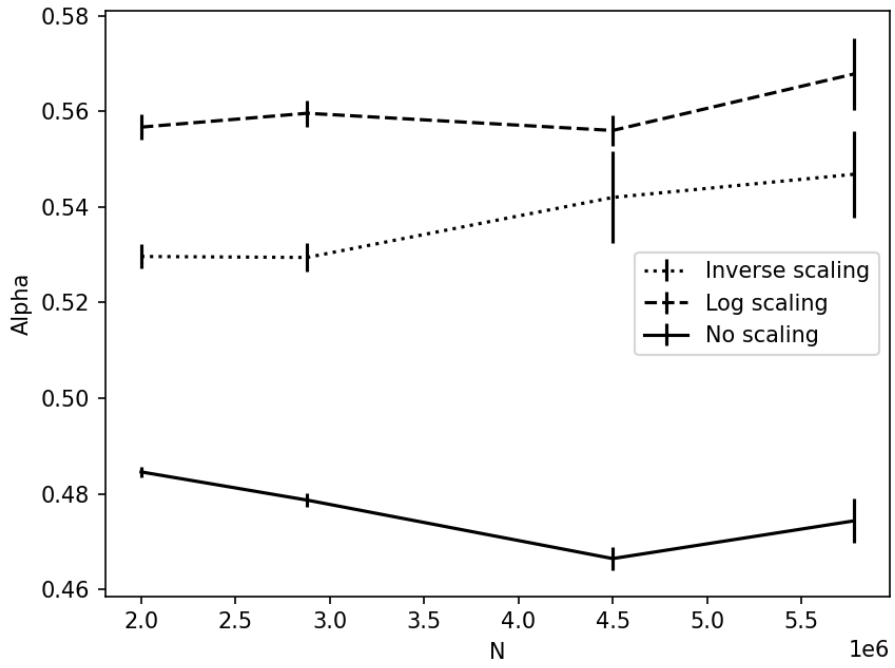

Figure 9: The optimal values of α as a function of the number of triangles N in the simulations that were compared to the simulations with the maximum number of triangles, for different rescaling techniques

As can be seen in figure 9, the three methods do not agree with each other within their respective errors. In these graphs, we expect to see a converging relation, as we

know that the correct value of α should be found as N goes to infinity. The result of the first method, without performing any extra rescaling on the axes besides the collapse itself, is significantly lower than the other two results, and has a significant different behaviour for high N. It therefore seems not close to being convergent for the chosen values of N. For this reason, we can conclude that this method indeed has to much emphasis on the data taken at the beginning of the simulation. This method is therefore left out of the rest of the results.

The other two methods are already much closer to each other, though they still do not agree. As pointed out in section 4.2, the method using the inverse should have the most emphasis on data with less statistical errors, and should for that reason give the best result. From figure 9, this seems indeed to be the curve closest to converging. At this point however, it is not possible to say more about which curve better approaches the true value of α. Therefore, for the final number of the critical exponent α the choice was made to take the weighted average of both results. This gives the final result

$$\alpha = 0.54 \pm 0.03. \tag{26}$$

The error is the systematic error, which is relatively large because of the high dependency on the method to measure α. There is also a statistical error, which comes from averaging over N and over the datasets from the Jackknife method, but it is negligibly small in comparison.

5.3 Visual checks on α

Now that we have a value for the critical exponent α, we can take a look at the collapses for it. In figure 10 the collapsed graphs can be seen for $\alpha = 0.54$. All three of the collapses look very neatly, though the graphs in figure 10c are not very smooth at high $tN^{-\alpha}$. This probably would be better in measurements with higher N, but as it is relatively not a very large part of the graph, it will not have much influence on the final result.

We can also visualise the triangulation for simulation times which are below and above τ for different values of N, to see if our approximation in figure 3 was correct and if there is indeed a visual difference between the triangulation below and above τ. This can all be summarised in figure 11, this shows the triangulation for different values of N, namely $N = 800$, $N = 3200$ and $N = 12800$, and different values of t. The triangulations are embedded in 2d, and all are shown in the same ratios. This gives an insight in how the triangulations are effected with increasing N. In the figure, the triangulation at $t = 0$ is what we would expect, the simple grid that the simulation starts with. At time t with $t \approx 0.2\tau$, the triangulation is clearly not a grid anymore, but still quite regular. Indeed, at small scales it gives the impression of a truly randomised triangulation, but at large scales it is still clearly regular. This is what was expected with the assumption made in figure 3. At $t = \tau$, the triangulation is completely randomised. This is especially visible as there are no clear visual differences between the pictures for the three different N at this point. It is also impossible to divide these pictures in circles as in figure 3, as they are not regular enough for this. This gives the impression that this number for α is indeed close to the true number that we would get for infinite N.

Now that we have found the critical exponent α, further research could look into decreasing the uncertainty on it by increasing the measurements, both in size and in quantity. The toy model could also be expanded to add extra dimensions. Hopefully, these results can teach us more about the geometry of our universe beyond the Planck scale.

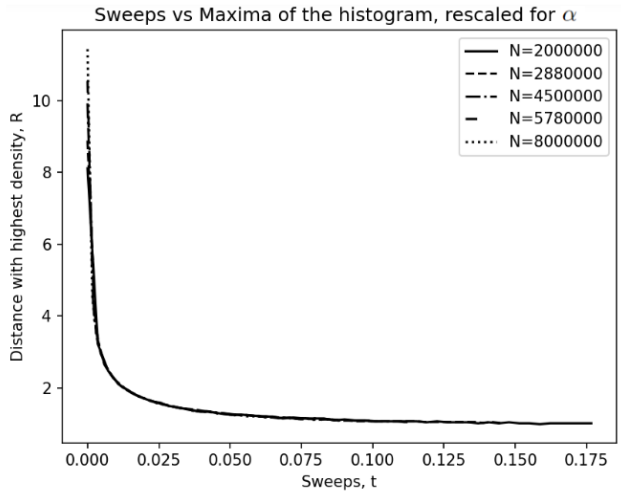

(a) No rescaling.

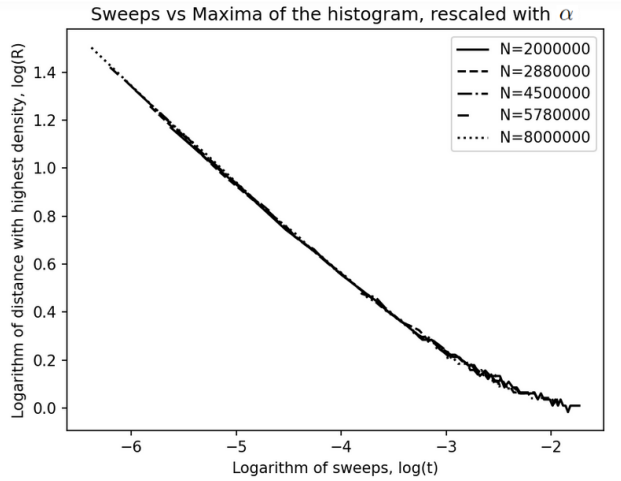

(b) Logarithmic scaling.

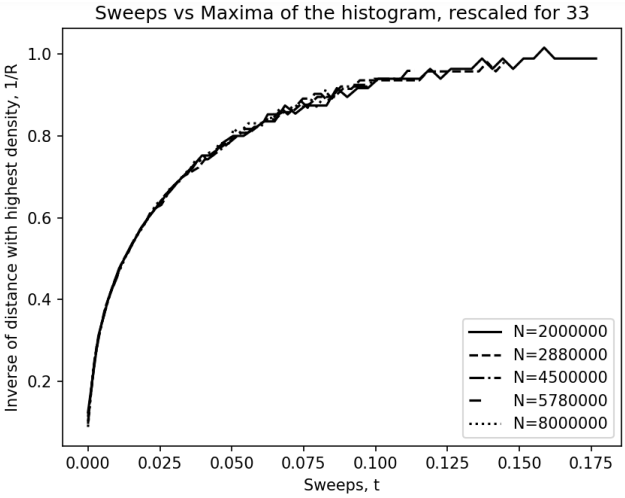

(c) Inverse scaling.

Figure 10: The collapse with $\alpha = 0.54$ of the graphs of the most probable distance between two random vertices for triangulation with N triangles after preforming t sweeps with different types of rescaling.

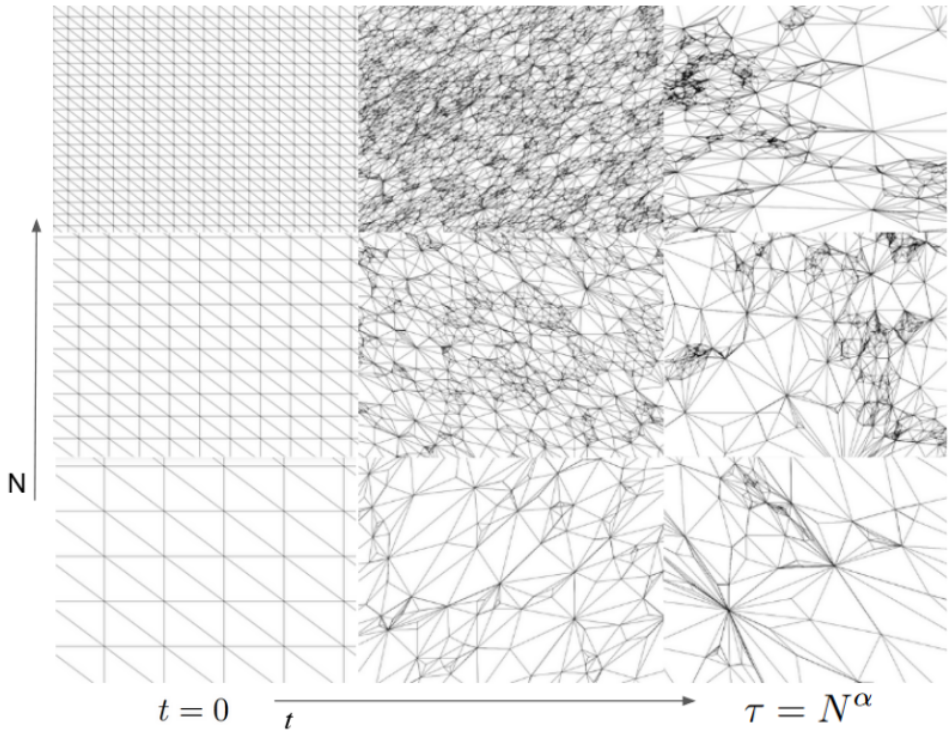

Figure 11: Example of plotted triangulations for three different amounts of N on three different amounts of sweeps, with α equal to the value computed in (26).

Acknowledgements

During the past few months I have learned a lot, both in a subject that was new to me and in programming. I would like to thank Timothy Budd for supervising me during this interesting project. It was incredibly helpful to be able to discuss my progress each weak. I would also like to thank Frank Filthaut for being the second reader of this thesis. Lastly, I would like to thank Bart Zonneveld for being my (tech)support and helping me figure out the difficult parts.

References

[1] Bernard Schutz. *Gravity from the ground up.* Cambridge University Press, 2003.

[2] Michael E. Peskin. *An Introduction To Quantum Field Theory.* Boca Raton, 1995.

[3] Timothy Budd. *Monte Carlo Techniques.* 2022.

[4] Timothy Budd. Non-perturbative quantum gravity: a conformal perspective. 2012.

[5] Djamel van der Sluis. Statistics of spatial geometries in causal dynamical triangulations in 2+1 dimensions. 2021.

[6] Manfredo Perdigao do Carmo and Francis J Flaherty. *Riemannian geometry.* 1992.

[7] W.J.P. Beenakker. *Reader for the course Quantum Field Theory.* 2020-2021.

[8] Assaf Shomer. A pedagogical explanation for the non-renormalizability of gravity, 2007.

[9] M Niedermaier. The asymptotic safety scenario in quantum gravity: an introduction. *Classical and Quantum Gravity*, 24(18), aug 2007.

[10] Victor Blacus. Running coupling constants for the electromagnetic, weak and strong interactions, 2016.

[11] Alessandra Caraceni and Alexandre Stauffer. Polynomial mixing time of edge flips on quadrangulations. 2018.

[12] Alessandra Caraceni. A polynomial upper bound for the mixing time of edge rotations on planar maps. *Electronic Journal of Probability*, 25, 2020.

[13] Thomas Budzinski. On the mixing time of the flip walk on triangulations of the sphere. pages 464–471, 2016.

[14] Jerome Barkley and Timothy Budd. Precision measurements of hausdorff dimensions in two-dimensional quantum gravity. *Classical and Quantum Gravity*, 36(24), nov 2019.

[15] Avery McIntosh. The jackknife estimation method. 2016.

[16] J. Kiefer. Sequential minimax search for a maximum. *Proceedings of the American Mathematical Society*, 4, 1953.

[17] Kari Rummukainen. Monte Carlo simulations in physics.